

## Supporting Information

# Which biopolymers are better for the fabrication of multilayer capsules? A comparative study using vaterite CaCO<sub>3</sub> templates

*Jack Campbell<sup>1</sup>, Jordan Abnett<sup>1</sup>, Georgia Kastania<sup>1</sup>, Dmitry Volodkin<sup>1\*</sup> and Anna*

*Vikulina<sup>2\*</sup>*

<sup>1</sup>Department of Chemistry and Forensics, School of Science and Technology,

Nottingham Trent University, Clifton Lane, Nottingham NG11 8NS, UK.

<sup>2</sup>Fraunhofer Institute for Cell Therapy and Immunology, Branch Bioanalytics and

Bioprocesses, Am Mühlenberg 13, 14476 Potsdam-Golm, Germany.

\*Correspondence: [dmitry.volodkin@ntu.ac.uk](mailto:dmitry.volodkin@ntu.ac.uk) (Tel: +44-115-848-3140, the UK);

[anna.vikulina@izi-bb.fraunhofer.de](mailto:anna.vikulina@izi-bb.fraunhofer.de) (Tel.: +49-331 58187-122, Germany).

**Table S1.** pKa and isoelectric point values for polymers and proteins used in this study, respectively. HA - Hyaluronic acid, CS - chondroitin sulphate, DS - dextran sulphate, HS - heparin sulphate, PLL - poly-L-lysine, PR - protamine, DA - dextran amine, COL - collagen.

Polymer	Isoelectric point (proteins)/pKa (polymers)	Ref
HA	3-4	[1]
CS	2-4	[2,3]
DS	2	[4]
HS	1-4	[5,6]
PLL	9-10	[7,8]
PR	12-13	[9]
DA	Unknown	
COL	7-9	[10,11]

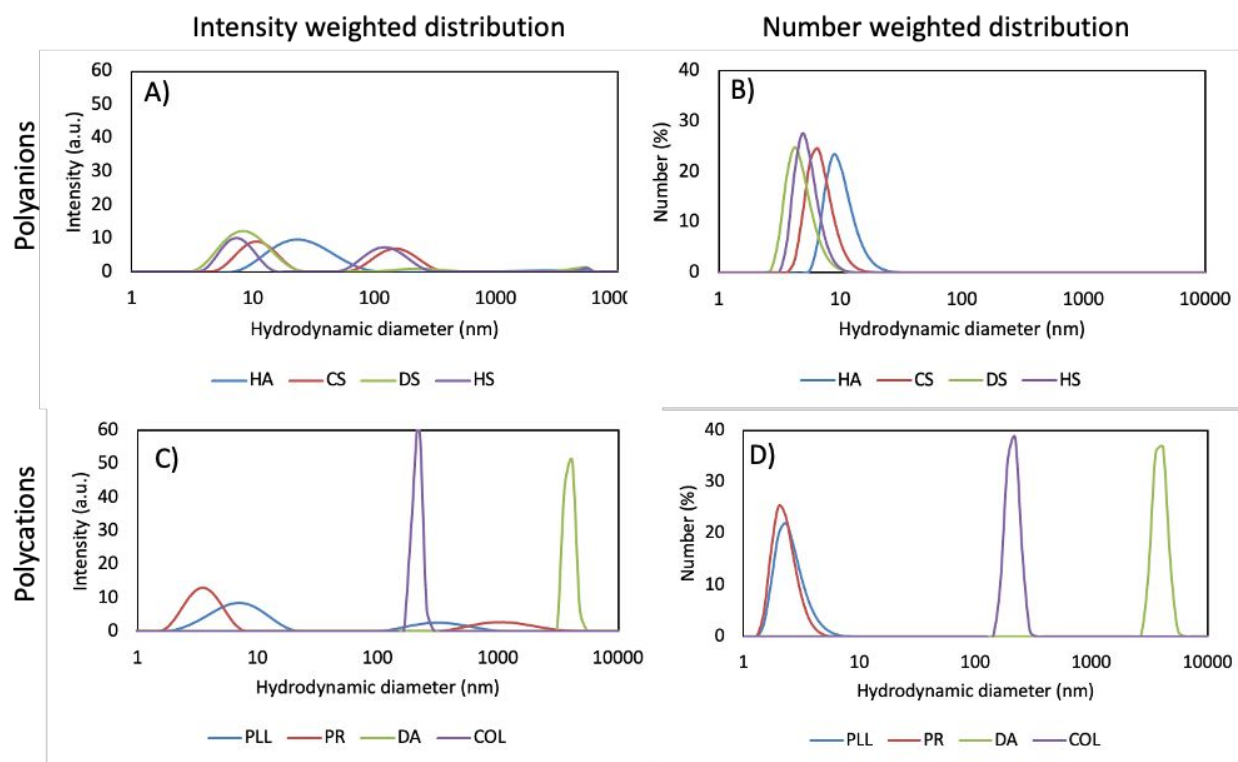


**Figure S1.** Intensity weighted and number weighted distributions for polyanions (A and B, respectively) and polycations (C and D, respectively).

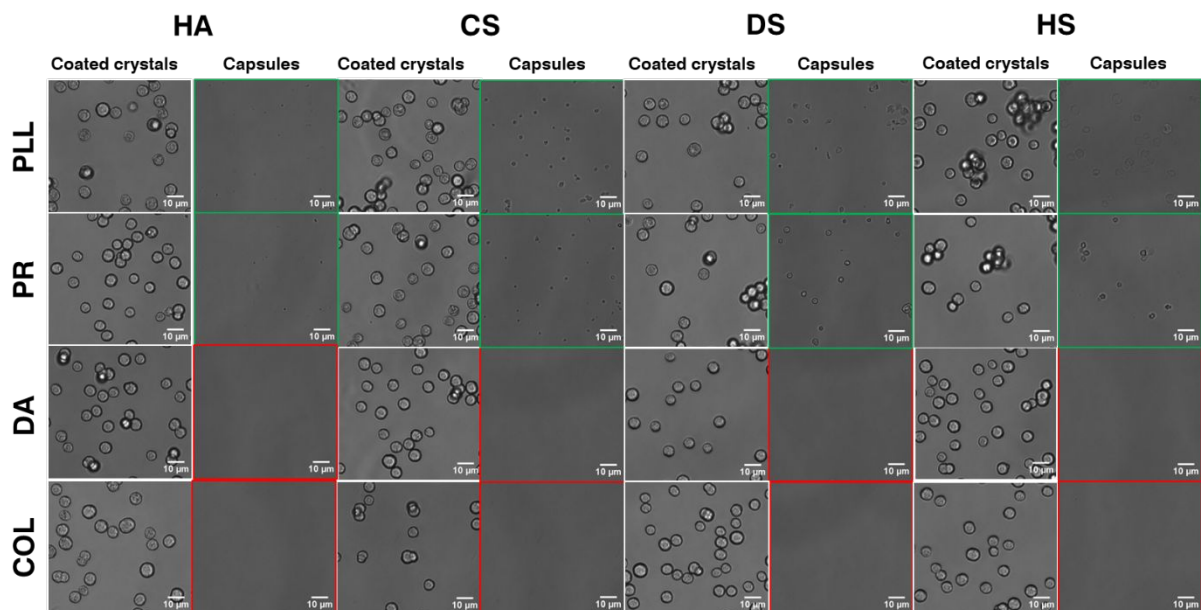


**Figure S2.** Transmittance images of (polyanion/polycation)<sub>2.5</sub> coated crystals and (polyanion/polycation)<sub>2.5</sub> capsules formed by dissolution of CaCO<sub>3</sub> cores by addition of 50 mM EDTA. 5 mM TRIS containing 27 mM NaCl 10 mM CaCl<sub>2</sub> with pH 7.9 has been used as a buffer solution throughout the experiment. Diameter of coated crystals is 7.5 ± 0.8 μm.

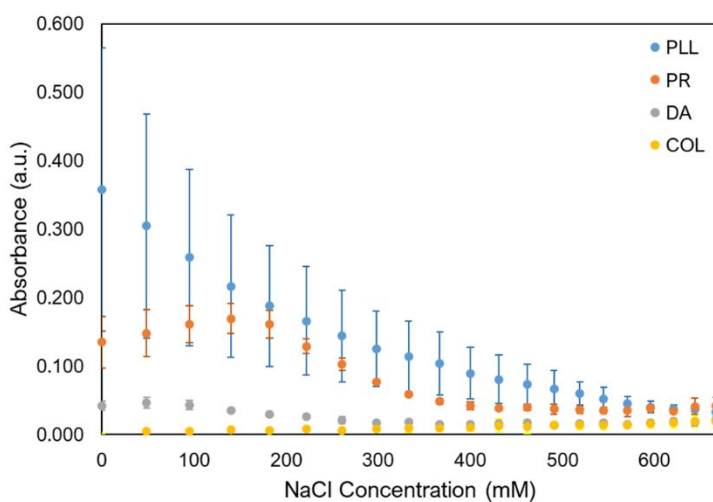


**Figure S3.** Turbidimetric titration of PECs made of CS and PLL, PR, COL or DA and formed in TRIS buffer solution pH 7.9. Initial concentration of NaCl is subtracted, x-axis represents added amount of NaCl.

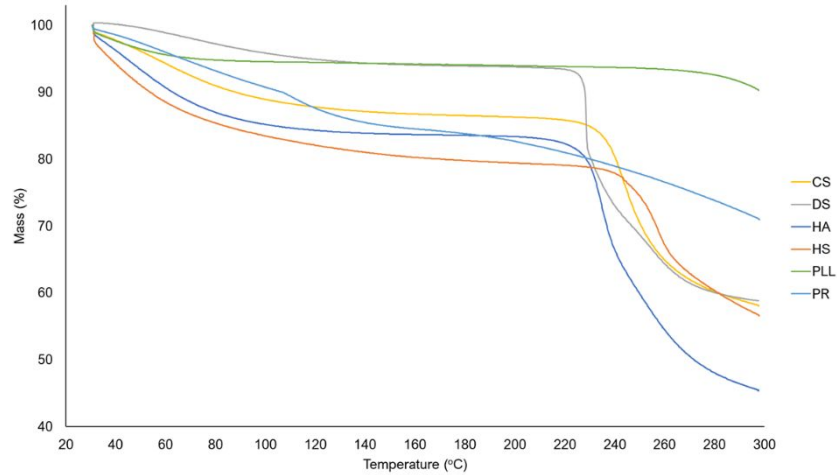


**Figure S4.** TGA curves of biopolymers that have formed stable capsules. Pure powdered polymer was heated from 30°C to 300°C at a rate of 10°C min<sup>-1</sup> under a helium atmosphere.

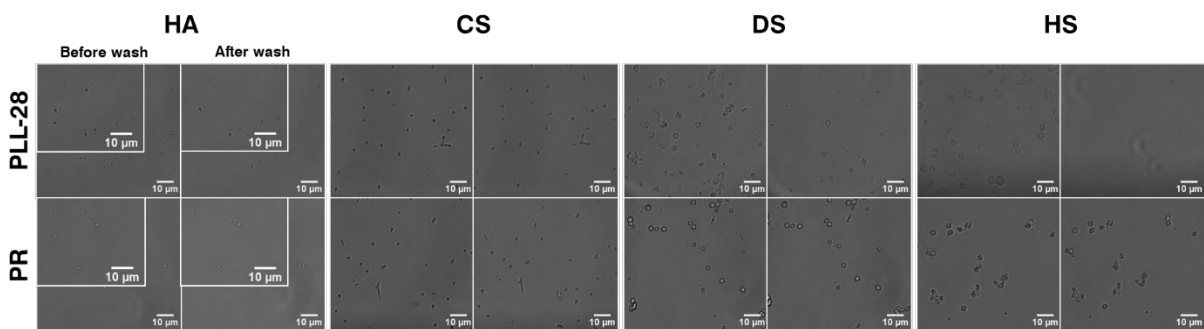


**Figure S5.** Optical transmittance images of formed PLL- and PR-based capsules. CaCO<sub>3</sub> cores are dissolved by addition of 50 mM EDTA. Surface adhering abilities of capsules is shown through images of the same positions; before (left) and after (right), after repeated washing steps with 5 mM TRIS containing 27 mM NaCl 10 mM CaCl<sub>2</sub> with pH 7.9.

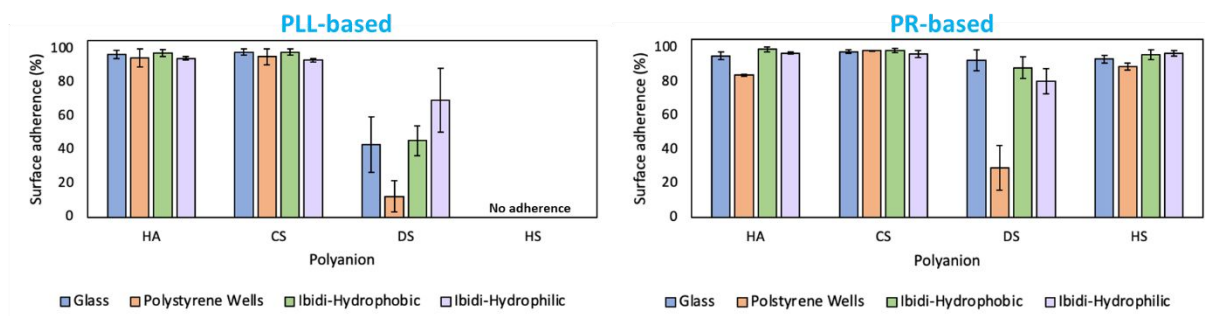


**Figure S6.** Adherence of PLL- and PR- based capsules on different surfaces (specified in a legend).  $\text{CaCO}_3$  cores have been dissolved by addition of 50 mM EDTA. Diameter of coated crystals is  $7.5 \pm 0.8 \mu\text{m}$ . Surface adhering abilities of capsules is calculated after repeated washing steps with 5 mM TRIS containing 27 mM NaCl 10 mM  $\text{CaCl}_2$  with pH 7.9, taking initial number of capsules as 100%. Error bars are S.D. for at least  $n = 100$  measurements.

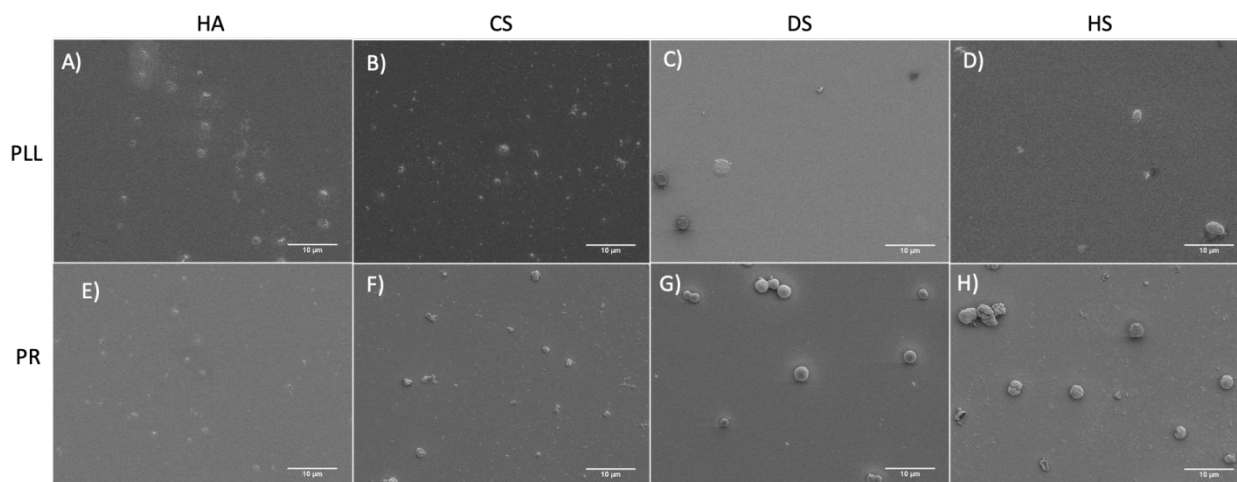


**Figure S7.** SEM images of 10 nm gold-sputtered capsules consisting of 2.5 bilayers. PLL-based (top row) capsules consisting of HA, CS, DS and HS are shown in images A), B), C), and D), respectively. PR-based (bottom row) capsules, consisting of HA, CS, DS and HS are shown in images E), F), G), and H), respectively. Scale bars are  $10 \mu\text{m}$ .

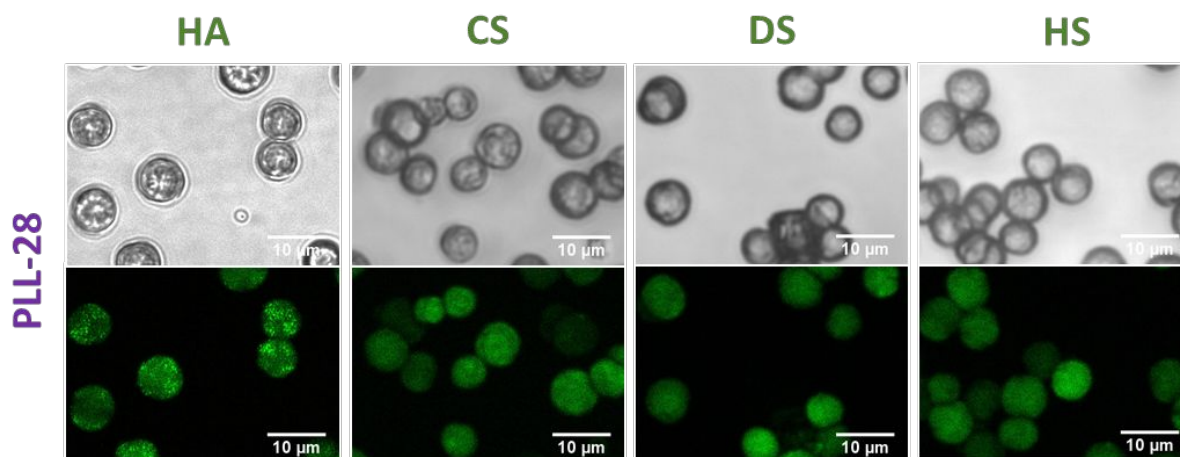


**Figure S8.** Confocal images of  $(\text{HA}^{\text{FITC}}/\text{PLL})_{2.5}$ ,  $(\text{CS}^{\text{FITC}}/\text{PLL})_{2.5}$ ,  $(\text{DS}^{\text{FITC}}/\text{PLL})_{2.5}$  and 4)  $(\text{HS}/\text{PLL}^{\text{FITC}})_{2.5}$  coated vaterite crystals (before dissolution of the core) Bright field (top) and fluorescence (excitation at 488 nm) (bottom) images. Capsules are prepared on  $\text{CaCO}_3$  cores of  $9 \pm 3 \mu\text{m}$  in diameter.

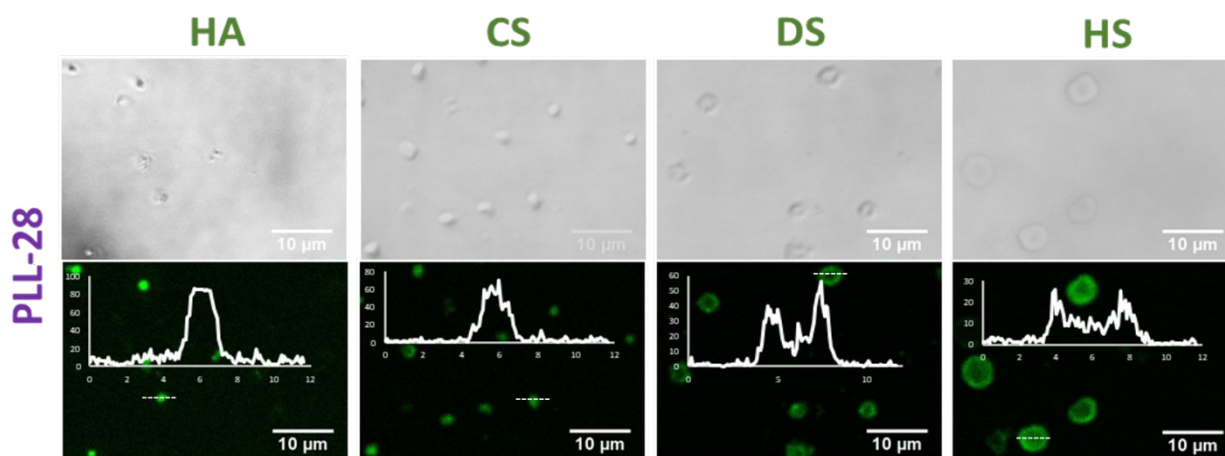


**Figure S9.** Confocal images of  $(\text{HA}^{\text{FITC}}/\text{PLL})_{2.5}$ ,  $(\text{CS}^{\text{FITC}}/\text{PLL})_{2.5}$ ,  $(\text{DS}^{\text{FITC}}/\text{PLL})_{2.5}$  and 4)  $(\text{HS}/\text{PLL}^{\text{FITC}})_{2.5}$  capsules after core dissolution. Capsules are prepared on  $\text{CaCO}_3$  cores of  $9 \pm 3 \mu\text{m}$  in diameter.  $\text{CaCO}_3$  cores are dissolved by addition of 50 mM EDTA. Bright field images (top) and fluorescence images (excitation at 488 nm) with corresponding linear fluorescence profiles across the middle of representative capsules (bottom). The white dashed line indicates how the line profile was taken.

1. Mero, A.; Campisi, M. Hyaluronic Acid Bioconjugates for the Delivery of Bioactive Molecules. *Polymers*. **2014**, *6* (1), 346–369. <https://doi.org/10.3390/polym6020346>.
2. Fajardo, A. R.; Lopes, L. C.; Valente, A. J. M.; Rubira, A. F.; Muniz, E. C. Effect of Stoichiometry and PH on the Structure and Properties of Chitosan/Chondroitin Sulfate Complexes. *Colloid Polym. Sci.* **2011**, *289*, 1739–1748. <https://doi.org/10.1007/s00396-011-2497-6>.
3. Seog, J.; Dean, D.; Plaas, A. H. K.; Wong-Palms, S.; Grodzinsky, A. J.; Ortiz, C. Direct Measurement of Glycosaminoglycan Intermolecular Interactions via High-Resolution Force Spectroscopy. *Macromolecules* **2002**, *35* (14), 5601–5615. <https://doi.org/10.1021/ma0121621>.
4. Gnanadhas, D. P.; Ben Thomas, M.; Elango, M.; Raichur, A. M.; Chakravortty, D. Chitosan-Dextran Sulphate Nanocapsule Drug Delivery System as an Effective Therapeutic against Intraphagosomal Pathogen Salmonella. *J. Antimicrob. Chemother.* **2013**, *68* (11), 2576–2586. <https://doi.org/10.1093/jac/dkt252>.
5. Wang, H. M.; Loganathan, D.; Linhardt, R. J. Determination of the PK(a) of Glucuronic Acid and the Carboxy Groups of Heparin by <sup>13</sup>C-Nuclear-Magnetic-Resonance Spectroscopy. *Biochem. J.* **1991**, *278* (3), 689–695. <https://doi.org/10.1042/bj2780689>.
6. Bhaskar, U.; Hickey, A. M.; Li, G.; Mundra, R. V.; Zhang, F.; Fu, L.; Cai, C.; Ou, Z.; Dordick, J. S.; Linhardt, R. J. A Purification Process for Heparin and Precursor Polysaccharides Using the PH Responsive Behavior of Chitosan. *Biotechnol. Prog.* **2015**, *31* (5), 1348–1359. <https://doi.org/10.1002/btpr.2144>.

7. Eckenrode, H. M.; Dai, H. L. Nonlinear Optical Probe of Biopolymer Adsorption on Colloidal Particle Surface: Poly-L-Lysine on Polystyrene Sulfate Microspheres. *Langmuir* **2004**, *20* (21), 9202–9209. <https://doi.org/10.1021/la048863j>.
8. Volodkin, D.; Ball, V.; Schaaf, P.; Voegel, J. C.; Mohwald, H. Complexation of Phosphocholine Liposomes with Polylysine. Stabilization by Surface Coverage versus Aggregation. *Biochim. Biophys. Acta* **2007**, *1768* (2), 280–290. <https://doi.org/10.1016/j.bbamem.2006.09.015>.
9. Xue, F.; Liu, L.; Mi, Y.; Han, H.; Liang, J. Investigation the Interaction between Protamine Sulfate and CdTe Quantum Dots with Spectroscopic Techniques. *RSC Adv.* **2016**, *6* (13), 10215–10220. <https://doi.org/10.1039/c5ra16586e>.
10. Hattori, S.; Adachi, E.; Ebihara, T.; Shirai, T.; Someki, I.; Irie, S. Alkali-Treated Collagen Retained the Triple Helical Conformation and the Ligand Activity for the Cell Adhesion via A2 $\beta$ 1 Integrin. *J. Biochem.* **1999**, *125* (4), 676–684. <https://doi.org/10.1093/oxfordjournals.jbchem.a022336>.
11. Meyer, M. Processing of Collagen Based Biomaterials and the Resulting Materials Properties. *Biomed. Eng. Online* **2019**, *18* (24). <https://doi.org/10.1186/s12938-019-0647-0>.